Astron. Astrophys. 320, 159–166 (1997)

ASTRONOMY
AND
ASTROPHYSICS

A search for clustering around Herbig Ae/Be stars

Leonardo Testi[1], **Francesco Palla**[2], **Timo Prusti**[3], **Antonella Natta**[2], **and Silvia Maltagliati**[1]

[1] Dipartimento di Astronomia e Scienza dello Spazio, Università degli Studi di Firenze, Largo E. Fermi 5, I-50125 Firenze, Italy
[2] Osservatorio Astrofisico di Arcetri, Largo E. Fermi 5, I-50125 Firenze, Italy
[3] Astrophysics Division, Space Science Department, ESTEC, Postbus 299, 2200 AG Noordwijk, The Netherlands

Received 13 November 1995 / Accepted 18 September 1996

Abstract. We present the results of new near-infrared observations of the fields around a sample of 19 Herbig Ae/Be stars. The observations reveal the population of young stars that accompanies the formation of intermediate-mass stars.

The richness of the detected star clusters is investigated. We find a clear dependence of the richness of the cluster on the spectral type of the Herbig Ae/Be star, confirming that the mode of formation of intermediate-mass stars represents the transition between the high-mass and the low-mass modes. In particular, we find that the cluster nature of star formation appears at a significant (i.e. detectable) level for stars of B7 spectral type or earlier.

Key words: stars: formation – stars: pre-main sequence – infrared: stars – open clusters: general

1. Introduction

It is a well established result that many stars do not form in isolation; young stars are usually found to be members of clusters or associations (see e.g. Lada et al. 1993; Zinnecker et al. 1993). Similarly, even apparently isolated low mass pre-main-sequence stars form small groups with densities of 10-100 stars per cubic parsec (Gomez et al. 1993). At the other extreme, high mass stars are associated with rich clusters with densities up to 10^4 objects per cubic parsec, as in the Trapezium cluster (McCaughrean and Stauffer 1994). Here and in the following we will call "in loose groups" or "in aggregates" the low-mass star formation mode, in analogy with the study of Gomez et al. (1993). Typical scales of this mode of formation are: a mean projected separation between the young stars of 0.3 pc and groups of ~ 15 stars within $0.5 - 1$ pc. On the opposite side, the term "cluster mode" does not imply a gravitationally bound system, but a group of stars from several tens to a few hundreds distributed over a scale $\lesssim 0.5$ pc, as observed in high-mass star forming regions like Orion (McCaughrean and Stauffer 1994).

Send offprint requests to: L. Testi

Herbig Ae/Be stars should represent the transition between the high-mass star formation mode in clusters and the low mass-mode in loose groups. In recent years, the evidence that the clustering effect begins at intermediate mass level has been found in several studies at optical and infrared wavelength (Barsony et al. 1991; Hillenbrand 1994; Palla et al. 1995). In spite of the fact that the near infrared wavelengths are the ideal choice for the study of the embedded population of young stars around Herbig Ae/Be stars, the literature on the subject is still scant (see however Hillenbrand 1995).

Li et al. (1994) performed near infrared imaging of 16 Herbig Ae/Be stars. Their primary goal was to investigate the possibility that diffuse circumstellar emission and nearby companions would have affected the large beam photometry of Herbig stars. For this reason the study was limited to a small area around the Herbig star itself (few tens of arcsec), and to the brigthest and closest companions.

In this paper, we report the results of wide-field and deep images in the broad-band near-infrared (NIR) filters J,H, and K of large (4–7 arcmin) fields around 19 Herbig Ae/Be stars. The NIR data (especially the K-band) are expected to reveal stars undetectable at optical wavelengths, enabling a detailed study of the embedded population of young stellar objects. As we will show below, although the present sample is still limited, the data clearly indicate the existence of a correlation between the stellar density of the fields and the spectral type of the Herbig star.

2. Observations

The nineteen Herbig stars of our sample have been selected with two criteria: (*i*) they should not be members of extended star forming complexes and (*ii*) they should cover a wide range of spectral types. These two requirements were set in order to study regions not affected by large scale star formation processes and to probe the dependence of the population of young stars on the spectral type of the target star.

In Table 1 we report the relevant parameters of the observed stars as obtained from the literature (Berrilli et al. 1992; Finkenzeller & Mundt 1984; Herbig & Bell 1988; Hillenbrand et al. 1992; Scarrot et al. 1986; Thè et al. 1994). The target stars

Table 1. Properties of the Herbig stars considered.

#	Star	R.A. (1950)	Dec. (1950)	Sp. type	Dist (pc)
1	LkHα 198	00 : 08 : 47.5	+58 : 33 : 05	A5	600
2	BD+61°154	00 : 40 : 21.9	+61 : 38 : 15	B8	650
3	RNO 6	02 : 13 : 03.0	+55 : 09 : 03	B1	1600
4	XY Per	03 : 46 : 17.4	+38 : 49 : 50	B6	160
5	AB Aur	04 : 52 : 34.2	+30 : 28 : 22	A0	160
6	UX Ori	05 : 02 : 00.6	−03 : 51 : 20	A2	450
7	HK Ori	05 : 28 : 40.1	+12 : 07 : 00	A4	450
8	T Ori	05 : 33 : 23.1	−05 : 30 : 26	A2	450
9	BF Ori	05 : 34 : 47.2	−06 : 36 : 45	A7	450
10	HD 37490	05 : 36 : 33.0	+04 : 05 : 00	B3	360
11	HD 250550	05 : 59 : 06.4	+16 : 30 : 59	B7	700
12	MWC 137	06 : 15 : 53.5	+15 : 18 : 09	B0	1300
13	LkHα 215	06 : 29 : 56.2	+10 : 11 : 51	B7	800
14	HD 259431	06 : 30 : 19.4	+10 : 21 : 38	B5	800
15	R Mon	06 : 36 : 26.1	+08 : 46 : 55	B0	800
16	LkHα 25	06 : 37 : 59.5	+09 : 50 : 53	B7	800
17	HD 52721	06 : 59 : 28.6	−11 : 13 : 41	B1	1150
18	LkHα 218	07 : 00 : 21.9	−11 : 21 : 46	B9	1150
19	BD+40°4124	20 : 18 : 42.7	+41 : 12 : 18	B2	1000

Table 2. Parameters of the Observations.

Star	Date	Field		Limiting Magnitude			Acc.	Abs. com.[a]
		($'$)	(pc)	J	H	K		M_K
LkHα 198	15 Jan 1996	7 × 7	1.2 × 1.2	17.7	16.9	16.6	8%	6.7
BD+61°154	9 Jan 1993	4 × 4	0.76 × 0.76	16.4	16.0	15.7	20%	5.6
RNO 6	20 Jan 1996	7 × 7	3.3 × 3.3	17.6	16.8	16.3	5%	4.3
XY Per	20 Jan 1996	7 × 7	0.33 × 0.33	17.8	16.8	16.8	5%	9.8
AB Aur	8 Jan 1993	4 × 4	0.19 × 0.19	16.5	15.5	15.5	20%	8.5
UX Ori	15 Jan 1996	7 × 7	0.92 × 0.92	17.8	16.8	16.8	8%	7.5
HK Ori	8 Jan 1993	4 × 4	0.52 × 0.52	16.6	16.0	15.7	20%	6.4
T Ori	15 Jan 1996	7 × 7	0.92 × 0.92	17.4	16.2	16.0	8%	6.7
BF Ori	20 Jan 1996	7 × 7	0.92 × 0.92	17.8	16.7	16.6	5%	7.3
HD 37490	15 Jan 1996	7 × 7	0.73 × 0.73	17.7	16.6	16.6	8%	7.8
HD 250550	9 Jan 1993	4 × 4	0.81 × 0.81	16.5	15.7	15.7	20%	5.5
MWC 137	18 Jan 1996	7 × 7	2.6 × 2.6	17.4	16.5	16.5	7%	4.9
LkHα 215	11 Feb 1994	7 × 7	1.6 × 1.6	17.5	16.0	16.0	8%	5.5
HD 259431	12 Feb 1994	7 × 7	1.6 × 1.6	16.8	15.6	15.7	8%	5.2
R Mon	15 Jan 1996	7 × 7	1.6 × 1.6	17.9	16.8	16.6	8%	6.1
LkHα 25	11 Feb 1994	7 × 7	1.6 × 1.6	17.9	16.0	16.0	8%	5.5
HD 52721	20 Jan 1996	7 × 7	2.3 × 2.3	17.7	16.8	16.8	5%	5.5
LkHα 218	20 Jan 1996	7 × 7	2.3 × 2.3	17.7	16.4	16.5	5%	5.2
BD+40°4124	30 Sep 1993	7 × 7	2.0 × 2.0	17.3	16.1	16.0	10%	5.0

[a]) Completeness absolute magnitudes in K have been calculated from the K limiting magnitudes assuming the distance quoted in Table 1 (see text 2.1).

span a range of spectral types from A7 to B0, ensuring a good coverage of the intermediate mass range.

The observations were carried out using the Arcetri NIR camera ARNICA mounted at the 1.5 meter telescope TIRGO[1]. ARNICA is equipped with a NICMOS3 256×256 pixels array, the scale on the detector is 0.96 arcsecond per pixel. For a complete description of the instrument and of its performances at TIRGO see Lisi et al. (1995), Hunt et al. (1996a). The sources were observed during several observing runs in 1993, 1994, and 1996. The size of the observed field was in some cases $\sim 4\times4$ square arcmin with constant signal to noise ratio over the field, in other cases $\sim 7 \times 7$ square arcmin were imaged with poorer signal to noise ratio at the edges than at the center. All the sources

[1] The TIRGO telescope is operated by the C.A.I.S.M.I.–C.N.R., Firenze, Italy.

have been observed in the three J, H and K broad bands. In most cases the Herbig star itself is saturated in the images.

Table 2 summarizes the parameters of the observation of each field: in the first column is the name of the Herbig star, in the second the date of the observation, in the third and the fourth the field imaged (in arcminutes and in parsecs), in the fifth, sixth and seventh, the limiting magnitudes achieved (3 σ in 4 arcsec aperture) in each band, and in the last two the photometric calibration accuracy and the completeness absolute magnitude in K (see below). For the large fields the limiting magnitudes quoted are those measured at the edges of the mosaic, while in the central region they are about one magnitude fainter.

All the data reduction and analysis were performed using the IRAF[2] and the ARNICA software packages (Hunt et al. 1994). The raw images were median averaged in order to obtain the flat field images. After flat fielding the images were registered and combined to form the large mosaics. Aperture photometry was performed using the DAOPHOT package. A four arcsecond aperture was used in all fields.

The photometric calibration was achieved observing during each night a set of UKIRT faint standards (Casali et al. 1992) or of TIRGO standards (Hunt et al. 1996b). The standard stars were observed at similar airmasses as the sources of interest; hence, no correction for airmass was applied. As explained in Hunt et al. (1996a), the photometry of point sources in the first runs of the camera were position-dependent on the array; for this reason the photometric accuracy of the data taken during the January 93 run is of the order of $\sim 20\%$.

2.1. Source detection and completeness

In detecting all the point sources in the images, the DAOFIND algorithm has proven unreliable for the faintest stars. For this reason the lists of sources in each field were compiled "by hand" inspecting the images at different contrast levels. Accurate centering of each source was obtained with a gaussian fitting algorithm, before performing the photometry.

To be conservative we assumed our data to be complete down to one magnitude brighter than the limiting magnitude of each field (quoted in Table 2). For the large field mosaics the "edge" limiting magnitudes have been considered. In the last column of Table 2 the absolute K-band completeness magnitudes are reported, these have been calculated assuming the distances reported in Table 1.

3. Results

Even a quick look at the images shows that the fields present large variations. As an example, Fig. 1 shows that the fields around MWC 137 and HD 52721 are quite crowded, while those around UX Ori and BF Ori contain just a few stars. Whether this reflects the fact that some of the Herbig stars do have a large number of companions that formed together in a cluster/group whereas others formed almost alone, is the main subject of this paper and will be investigated in the following.

Due to the reduced amount of extinction, the K-band images are the the most suitable to reveal the embedded objects around the Herbig stars. For this reason the effects of variable extinction toward different fields, which may introduce significant errors at optical wavelengths, are expected to affect only marginally the results of our study.

The simple approach of counting the stars in each field cannot be used, since the target stars are located at different distances from the Sun and the sensitivity, as well as the total field of view of the observations, change from star to star. Moreover, the fields are located towards different regions of the galaxy, hence a different contamination from background objects is expected. In order to compensate for these effects, we will extract from the data a set of *indicators* of the clustering of stars around each Herbig star, and we will investigate the properties of such indicators.

3.1. Distance and sensitivity correction

Since our program stars are at different distances and the observations reach different sensitivity limits, the absolute K-band completeness magnitudes (assuming null extinction) are different. Thus, we have calculated one *indicator* ($\mathcal{N}_{\rm K}$) corrected for this effect: $\mathcal{N}_{\rm K}$ is the number of K-band sources detected with $M_{\rm K} < 5.2$ within 0.21 pc from the Herbig star. The physical radius of 0.21 pc was chosen because it is large enough to contain the clusters observed in BD+40°4124 and MWC 137, and at the same time is sufficiently small that only two of the nearest stars (AB Aur and XY Per) have been observed with a smaller field of view. Such a choice of the radius is also based on the results of Hillenbrand (1995) who fixed the effective size of the cluster at 0.17 pc. Due to the larger extent of our fields, we can be more conservative and take a larger value of the cluster size. The threshold at $M_{\rm K} = 5.2$ includes most of the fields (cf. Table 2, last column), but is high enough to be able to count some stars in most fields.

With this choice five fields have only lower limits of $\mathcal{N}_{\rm K}$. These fields are: MWC 137, RNO 6 and BD+40°4124, whose absolute completeness magnitude is lower than 5.2, and AB Aur and XY Per, which have been imaged with a field smaller than 0.21 pc. The values of $\mathcal{N}_{\rm K}$ for each star are reported in Table 3 (column 3).

3.2. Infrared excess sources

Since we are trying to find a way to separate the young stars around the Herbig stars from the foreground/background objects, the colour-colour diagram (J–H,H–K) could be a very useful tool. In fact main-sequence (MS) stars and reddened MS stars tend to lie in a different region of the (J–H,H–K) plane than young stars (Lada & Adams 1992). The latter usually show a marked NIR excess and are located to the right of the MS and reddened MS loci.

[2] IRAF is the Image Reduction and Analysis Facility made available to the astronomical community by the National Optical Astronomy Observatories, which are operated by AURA Inc., under contract with the U.S. National Science Foundation.

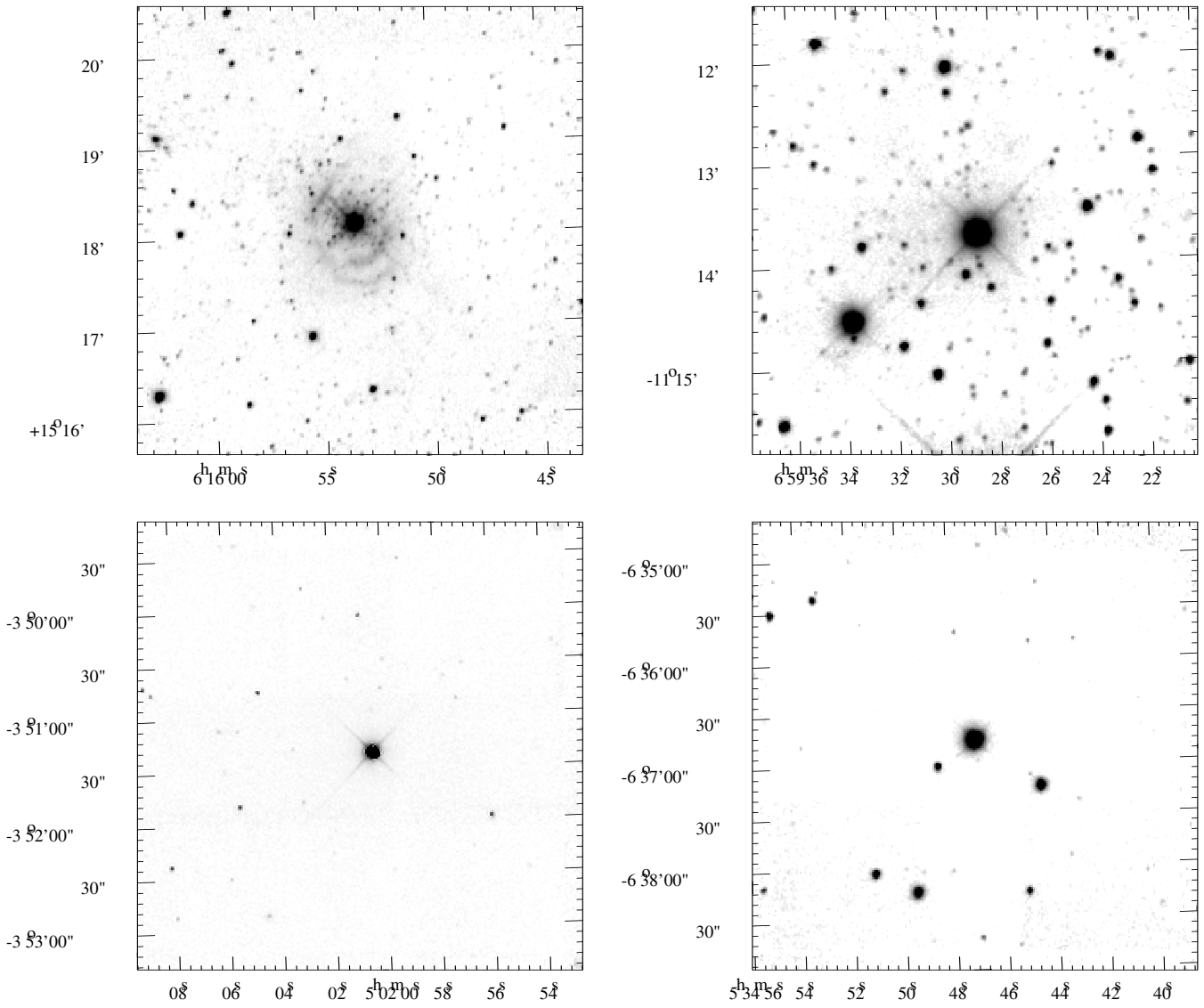

Fig. 1. K-band images of four Herbig stars: MWC 137 (upper left), HD 52721 (upper right), UX Ori (lower left) and BF Ori (lower right). On the axes are reported right ascension and declination for the 1950.0 epoch. Rich clusters are evident in MWC 137 and HD 52721, while the other two stars appear isolated.

A problem in using this method to discriminate between young stars (members of the cluster) and field stars, is that some kind of young stars (the Weak Line T-Tauri stars or in general the infrared Class III sources) do not show infrared excess at all. For example, about 50% of the known PMS stars in Taurus-Auriga fall within or very close the reddening band (Kenyon & Hartmann 1995). Also Class I sources have been found, in some cases, to fall inside the "reddening belt" (see e.g. Greene & Meyer 1995), and thus a fraction of them may not be easily detected in the colour–colour diagram. This means that using this method we may strongly underestimate the actual number of source members of the cluster around the Herbig star.

Notwithstanding these limitations, we define a *richness indicator*, $\mathcal{N}_{\rm EX}$, based on the colour properties of the sources: this quantity represents the number of NIR excess sources in each field with the same constraints as $\mathcal{N}_{\rm K}$, plus the requirement that each source should have been detected in all the three bands. A star is considered to have NIR excess if it satisfies the condition $(\mathrm{J}-\mathrm{H}) < 1.75(\mathrm{H}-\mathrm{K}) - 0.35$. This relation takes into account 10% error in the color determination. To give an estimate of the fraction of the sources detected in all the three bands that show infrared excess we have calculated $\mathcal{F}_{\rm EX}$ as the ratio of $\mathcal{N}_{\rm EX}$ to the number of sources detected in all the three bands (with the same constraints as for $\mathcal{N}_{\rm K}$). These two quantities are listed in column 4 and 5 of Table 3.

3.3. K-band sources density profiles

The indexes $\mathcal{N}_{\rm K}$, $\mathcal{N}_{\rm EX}$ and $\mathcal{F}_{\rm EX}$ are still not corrected for the contamination from background/foreground stars, which may

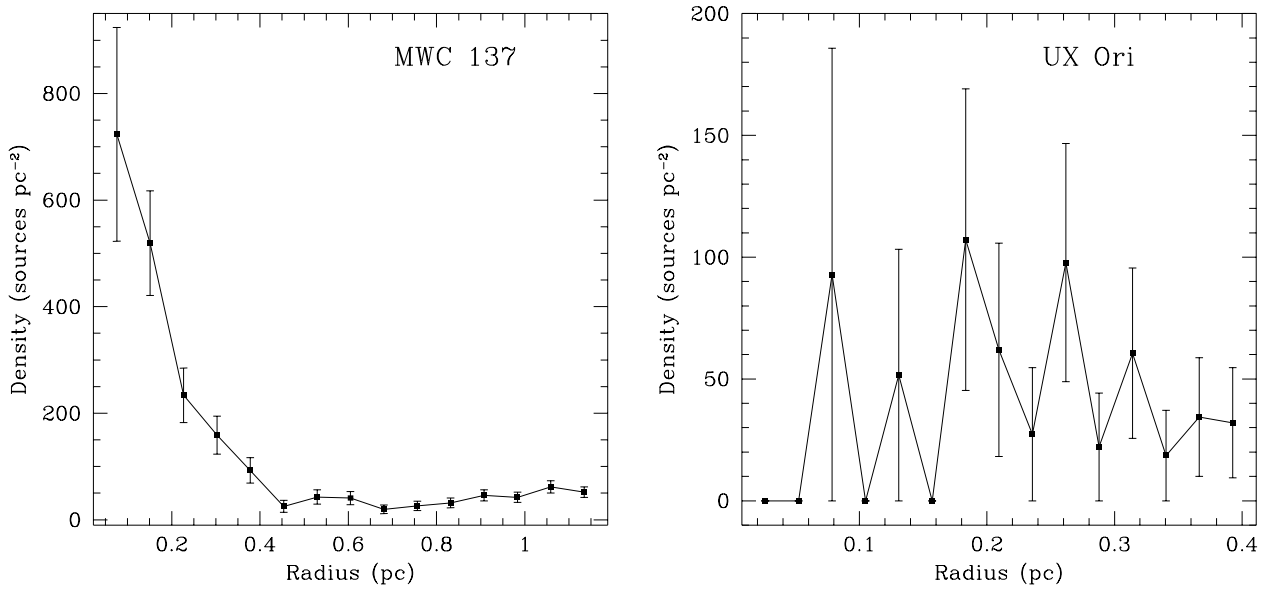

Fig. 2. Two examples of sources density profiles, on the left a rich cluster field, on the right an empty field. The error bars represent the statistical uncertainties.

affect fields at different galactic latitude and longitude in different ways. We have tried to account for this effect using the predictions of analytic star counts models. In particular, we have used the model of Ortiz & Lépine (1993), but with little success. The relatively small fields surveyed and the "local" small-scale extinction enhancement (not considered in the models) lead to great uncertainties in the predicted background/foreground star counts and we have decided that the results of such analysis were not meaningful.

A more straightforward way of estimating the amount of contamination is by plotting the stellar surface density in the K-band for each field as a function of the distance from the Herbig star. In practice, the local source density at radius r_i has been measured from the position of the Herbig star (see Table 1) in annuli of $12''$. As a result, it is found that there are some fields in which the Herbig star is located near the center of a marked local star density enhancement, while in other cases the density is almost constant across the whole field. In Fig. 2 two extreme cases are shown: the richest cluster associated with MWC 137 and an empty field around UX Ori.

More formally, we define another *richness indicator* of the cluster around each star as the number of sources in the density enhancement, $I_C = 2\pi \int_0^\infty r(n(r) - n_\infty)dr$, where $n(r)$ is the density of stars at radius r and $n_\infty = \lim_{r\to\infty} n(r)$. Practically, we will define n_∞ as the mean density in the outer parts of the plot, and $I_C = \pi \sum_{i=1}^{imax}(r^2_i - r^2_{i-1})(n(r_i) - n_\infty)$ ($r_0 = 0$, and r_{imax} is chosen in such a way to contain all the cluster members in the field). Table 3 lists the values of I_C in each field (column 6).

In principle, I_C is a very good indicator, since the contribution from field stars is evaluated close to the cluster area and subtracted before the integration. On the other hand, the correct determination of n_∞ is critical for the quantitative result, as shown by the error on I_C quoted in Table 3 and reported in Fig. 4, which has been determined by propagating the uncertainty in the determination of n_∞ on the sum defined above.

Two possible sources of systematic errors in the comparison of the values of I_C in different fields are: (i) the fact that all the sources detected within the completeness of each observations have been considered and (ii) the extinction toward each of the fields may differ by several magnitudes. Unfortunately the low number of stars around the sources does not allow a meaningful determination of the source densities maintaining the constraint of the same absolute limiting magnitude in all the fields. Nevertheless, we do not find a correlation between the absolute completeness magnitudes and the presence of a star cluster. For instance, HD 37490 and HD 52721 have absolute completeness magnitudes that differ by more than two magnitudes, but the cluster appearence and the value of I_C are similar.

The effect of extinction is more difficult to estimate, because of the uncertainties in the determination of this quantity from the NIR data alone. On the other hand, since n_∞ is calculated around the cluster, only the "local" extinction variations on the same scale of the clusters may affect the calculation of I_C. Hillenbrand et al. (1995) used the measured column densities of molecular gas to get an estimate of the extinction effect toward different fields. She found variations in extinction as large as ten magnitudes in the visual, but she also noted that the amount of extinction is not correlated with the spectral type. Thus, we can conclude that while this effect may affect the direct comparison of some fields, it should not alter the general trend in I_C that we find and that will be discussed below.

Finally, we like to stress that in all the cases in which a well defined cluster has been found, the bulk of the cluster is within 0.21 pc from the Herbig star. This result confirms the goodness of our choice of the physical size in the calculation of $\mathcal{N}_K$. In two

cases, LkHα 198 and R Mon, the value of I_C is highly negative, indicating that n_∞ is much greater than the density around the Herbig star. There are two possible explanations for this result: one is that when the Herbig star is very bright and with an extended nebulosity, as in the case of LkHα 198, nearby faint stars may be hidden, and be completely missed in our counts. Another possibility is the presence of a compact molecular clump around the star that enhances the value of the extinction along the line of sight close to the star and that obscures background objects. Clearly, further observations of these two regions are needed in order to understand what is the actual situation in these special cases.

4. Correlation between the richness indicators and the spectral type

Having defined suitable richness indicators, we can now study their dependence on the spectral type of the Herbig stars. We have decided to use the spectral type and not the mass of the star (which would be the physical quantity of relevance) for several reasons. The most important is that the determination of the mass is always indirect and relies on the use of HR diagrams. Although the knowledge of the PMS evolution has improved lately (Palla & Stahler 1993), the uncertainty with which both the distance and the luminosity of the Herbig stars are known is still too large to allow any reliable mass estimate using classical methods of stellar evolution. Unlike the mass, the spectral types of Herbig stars are known sufficiently well: the typical error found in the literature is of only one or two subclasses.

Table 3 reports the values of the *richness indicators* in each of the observed fields. The fields have been sorted by the spectral type of the Herbig star. In Figs. 3 and 4 the *richness indicators* have been plotted against the spectral type of the central star. We do not show the error bar in the spectral type since it is the same for all the stars of the sample.

A first result from Fig. 3 is that $\mathcal{N}_K$, $\mathcal{N}_{EX}$ and $\mathcal{F}_{EX}$ show a rough correlation with the spectral type, with earlier types having higher values of the *indicators*. MWC 137, which is the Herbig star with the earlier spectral type (B0) in our sample shows the highest values of the *richness indicators*. The only early type B star for which all the indicators give negative results is R Mon.

From Table 3, low-mass Herbig stars have $\mathcal{N}_K \lesssim 4$, which corresponds to a density of about 100 stars per cubic parsec. This density is similar to that found by Gomez et al. (1993) around known TTauri stars in Taurus ($\lesssim 60$ stars per cubic parsec). B-type Herbig stars have mean density values of about $250 \div 500$ stars per cubic parsec, but in the case of MWC 137 the density is 1.5×10^3 stars per cubic parsec, a value typical of massive star forming regions.

Our results are very similar to those obtained by Hillenbrand (1995) for seventeen fields around Herbig Ae/Be stars. In particular, she finds that the local density of K-band sources spans from a few tens per square parsecs for the fields around low-mass stars to several hundreds for those around high-mass stars. There are eight Herbig stars that are common to the two surveys. Considering the differences in the completeness limit and region surveyed of the two studies, the agreement in the numerical values of $\mathcal{N}_K$ for the fields in common is quite satisfactory.

Table 3. Values of the *richness indicators* in each field.

Star	*type*	$\mathcal{N}_K$	$\mathcal{N}_{ex}$	$\mathcal{F}_{EX}$	I_C
MWC 137	B0	59^a	26^a	0.55^a	76.0 ± 9
R Mon	B0	0	–	–	-12.8 ± 3
HD 52721	B1	10	–	–	20.5 ± 4
RNO 6	B1	11^a	3^a	0.5^a	11.0 ± 1
BD+40°4124	B2	19^a	12^a	0.75^a	11.0 ± 3
HD 37490	B3	9	6	0.75	9.9 ± 3
HD 259431	B5	2	–	–	0.9 ± 2
XY Per	B6	3^a	$-^a$	$-^a$	11.3 ± 3
LkHα 25	B7	11	2	0.18	14.5 ± 5
LkHα 215	B7	7	6	1.0	3.9 ± 1
HD 250550	B7	4	–	–	2.2 ± 2
BD+61°154	B8	8	1	0.13	-1.4 ± 3
LkHα 218	B9	8	1	0.14	2.0 ± 5
AB Aur	A0	0^a	$-^a$	$-^a$	1.2 ± 1
UX Ori	A2	0	–	–	-0.3 ± 1
T Ori	A2	5	–	–	1.0 ± 1
HK Ori	A4	7	–	–	2.2 ± 1
LkHα 198	A5	6	–	–	-10.6 ± 11
BF Ori	A7	4	–	–	1.1 ± 1

[a]) The values of the *indicators* for these sources are only lower limits.

The best evidence for the existence of a trend in the clustering properties with the spectral type of the Herbig star is shown in Fig. 4 where we plot Ic vs. spectral type. Early type stars have values of I_C above ten, while late type stars are characterized by values of order unity. MWC 137 has the highest value of I_C. In terms of I_C, the clustering around the Herbig Be stars is revealed at a level of 5-10 "effective stars" above the background (note that I_C takes into account the different galactic background/foreground contamination suffered by the different fields). Considering the results of Hillenbrand (1995) and of Barsony et al. (1991), the sample of Herbig stars with rich clusters includes MWC 137, MWC 297, MWC 1080, BD+40°4124, and LkHα 101.

From our results, the variation of I_C with spectral type is not smooth. As shown in fig. 2, there is an indication of the possible presence of a threshold (or sudden break) effect in I_C around a spectral type B5-B7. It is too early to say whether this effect is real or an artifact of our small sample of stars. Hillenbrand (1995) finds a linear relationship of the star density with the stellar mass. However, we have already warned about the large uncertainty in the mass assignment of the Herbig stars and the derived relation may suffer from this drawback. Judging from the behaviour of the indicator $\mathcal{N}_K$, a quantity more similar to that used by Hillenbrand than I_C , there is no evidence in our data for such a linear correlation (cf. Fig. 3). On the other hand, the existence of a *minimum* mass for the presence of clustering effects (also related to environmental conditions) would provide a strong constraint on star formation theories.

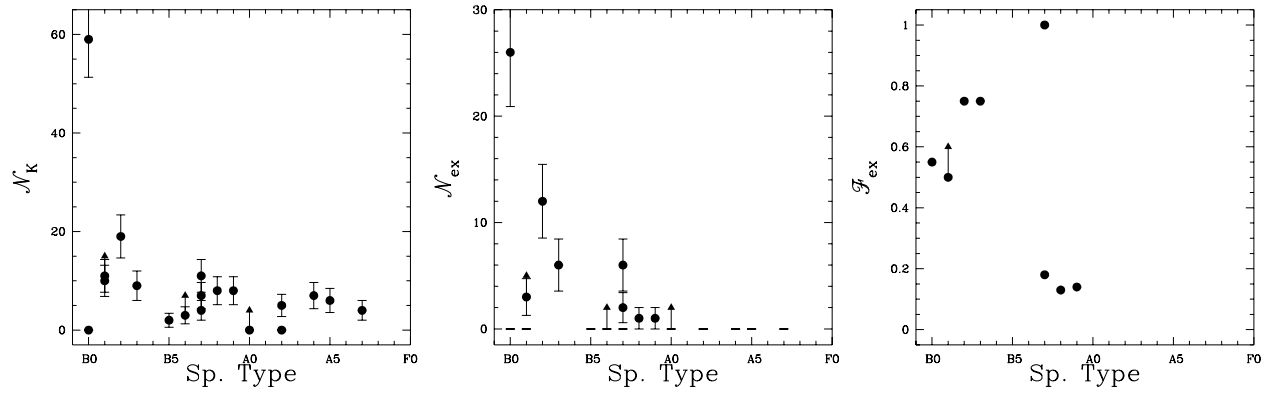

Fig. 3. *Richness indicators* versus spectral type of the Herbig star. On the left $\mathcal{N}_K$: sources detected in K band with $M_K \leq 5.2$ and within 0.21 pc from the Herbig star; center $\mathcal{N}_{EX}$: sources detected in all the three bands, with infrared excess, with $M_K \leq 5.2$ and within 0.21 pc from the Herbig star; on the right $\mathcal{F}_{EX}$: ratio between $\mathcal{N}_{EX}$ and the sources detected in all the three bands with $M_K \leq 5.2$ and within 0.21 pc from the Herbig star. The fields for which $\mathcal{N}_{EX} = 0$ have been represented with dashes in the central panel and have not been reported in the right panel. Lower limits are indicated with an arrow.

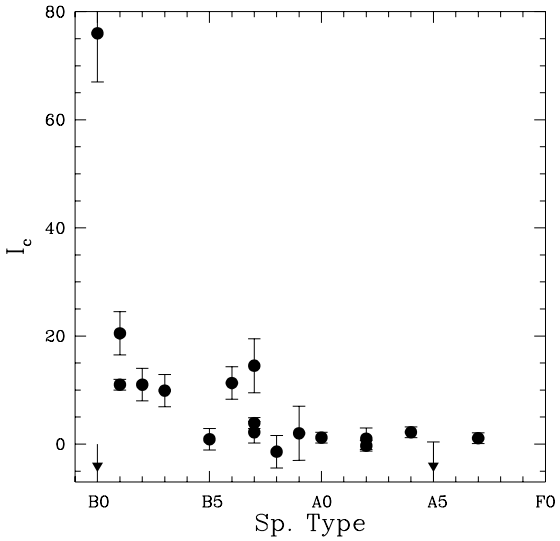

Fig. 4. The *richness indicator* I_C versus the spectral type of the Herbig star.

5. Conclusions

Although our data are limited to a subsample of the intermediate mass pre-main sequence Herbig Ae/Be stars, a few conclusions can be drawn from this study.

Our NIR images reveal the population of low-mass stars around Herbig Ae/Be stars, undetectable at shorter wavelengths (Goodrich 1993; Aspin et al. 1994; Hillenbrand et al. 1995). We have investigated the clustering of young stars around the target stars by means of several *richness indicators*. The main results of this analysis can be summarized in two points: 1) there is a clear dependence between the spectral type of the Herbig star and the richness of the embedded cluster around it: the earlier the spectral type, the richer the cluster; 2) the presence of clusters appears at a detectable level only for stars earlier than B5-B7. While the former result is supported by the study of Hillenbrand (1995) on a similar set of stars, the existence of a threshold spectral type (or, more physically, of a minimum mass) has to be verified on a larger sample, using a homogeneous *richness indicator*, such as I_C.

These initial results confirm the idea that the class of Herbig Be stars represents the transition between the isolated star formation mode, typical of low-mass stars, which includes Ae-type stars, and the rich cluster mode typical of high-mass O stars. These statements can be, and will be, made more precise as soon as observations of other stars of this class will become available. Ideally, Herbig Be stars are the most interesting candidates to study the appearance of associated clusters.

Acknowledgements. We thank the TIRGO and ARNICA staff, especially Filippo Mannucci and Ruggero Stanga, for nice scheduling and for service observing. LT acknowledges many interesting discussions with Thierry Montmerle and Paolo Saraceno, and would like to thank Jaques Lépine for useful suggestions and for providing the fortran code of the star counts model. We also thank the referee, Hans Zinnecker, whose suggestions greatly improved this work. This search has made use of the Simbad database, operated at CDS, Strasbourg, France.

References

Aspin, C., Sandell, G., Weintraub, D.A., 1994, A&A, 282, L25
Barsony, M., Schombert, J.M., Kis-Halas, K., 1991, ApJ, 379, 221
Berrilli, F., Corciulo, G., Ingrosso, G., Lorenzetti, D., Nisini, B., Strafella, F., 1992, ApJ, 398, 254
Casali, M., et al. 1992, UKIRT Internal Memorandum
Finkenzeller, U., & Mundt, R., 1984, A&AS, 55, 109
Greene, T.P., & Meyer, M.R., 1995, ApJ, 450, 233
Gomez, M., Hartmann, L., Kenyon, S.J., Hewett, R., 1993, AJ, 105, 1927
Goodrich, R.W., 1993, ApJS, 86, 499
Herbig, G.H., & Bell, K.R., 1988, Bullettin of the Lick Observatory n. 1111
Hillenbrand, L.A., 1995, Ph.D. Thesis, University of Massachusets

Hillenbrand, L.A., 1994, in *The Nature and Evolutionary Status of Herbig Ae/Be Stars*, P.S. Thé, M.R. Peréz & J.P.E. van den Heuvel eds., A.S.P. Conf. Ser., p.369
Hillenbrand, L.A., Meyer, M.R., Strom, S.E., 1995, AJ, 109, 280
Hillenbrand, L.A., Strom, S.E., Vrba, F.J., Keene, J., 1992, ApJ, 397, 613
Hunt, L.K., Lisi, F., Testi, L., Baffa, C., Borelli, S., et al., 1996a, A&AS, 115, 181
Hunt, L.K., Migliorini, S., Testi, L., Stanga, R.M., Aspin, C., et al., 1996b, AJ, submitted
Hunt, L.K., Testi, L., Borelli, S., Maiolino, R., Moriondo, G., 1994, Technical Report 4/94, Arcetri Astrophysical Observatory
Kenyon, S.J. & Hartmann, L. 1995, ApJS, 101, 117
Lada, C., & Adams, F.C., 1992, ApJ, 393, 278
Lada, E.A., Strom, K.M., Myers, P.C.,1993, in *Protostars and Planets III*, E.H. Levy & J.I. Lunine eds., (Tucson: The University of Arizona Press), p.245
Li, W., Evans, N.J.,II, Harvey, P.M., Colomé, C., 1994, ApJ, 433, 199
Lisi, F., Hunt, L.K., Baffa, C., Biliotti, V., Bonaccini, D., et al, 1995, PASP, 108, 364
McCaughrean, M.J., & Stauffer, J.R., 1994, AJ, 108, 1382
Montmerle, T., Feigelson, E.D., Bouvier, J, André, P.,1993, in *Protostars and Planets III*, E.H. Levy & J.I. Lunine eds., (Tucson: The University of Arizona Press), p.689
Ortiz, R., & Lépine, J.R.D., 1993, A&A, 279, 90
Palla, F., & Stahler, S.W. 1993, ApJ, 418, 414
Palla, F., Testi, L., Hunter, T.R., Taylor, G.B., Prusti, T., et al. 1995, A&A, 293, 521
Scarrot, S.M., Brosch, N., Ward-Thompson, D., Warren-Smith, R.F., 1986, MNRAS, 223, 505
Shu, F.H., Adams, F.C., & Lizano, S., 1987, ARAA, 25, 23
Thé, P.S., de Winter, D., & Pérez,M.R., 1994, A&AS, 104, 315
Zinnecker, H., McCaughrean, M.J., Wilking, B.A., 1993, in *Protostars and Planets III*, E.H. Levy & J.I. Lunine eds., (Tucson: The University of Arizona Press), p.429

This article was processed by the author using Springer-Verlag LaTeX A&A style file *L-AA* version 3.